CrossMark

RESEARCH ARTICLE

Electrochemical investigation of electrolyte composition and electrolysis parameters during zinc electrowinning

C. Su[1] · W. Zhang[1] · E. Ghali[1] · G. Houlachi[2]

Abstract The effect of different Mn^{2+} and Pb^{2+} concentrations added to the zinc sulfate acid electrolyte during zinc electrowinning process was investigated. Operating parameters such as zinc ion concentration, acid concentration, current density, electrolyte agitation, and temperature were investigated in the presence of Mn^{2+} and Pb^{2+}. Galvanostatic polarization, potentiodynamic polarization, cyclic voltammetry, and electrochemical impedance spectroscopy studies were performed to examine the cathodic behavior. Scanning electron microscopy (SEM) and X-ray diffraction (XRD) were employed to characterize the surface of the zinc deposit. The addition of lead ions to the zinc electrolyte led to an increase in the cathodic potential and current efficiencies of the zinc deposition. The addition of Mn^{2+} to the zinc electrolyte resulted in a decrease in the cathodic potential and current efficiency of zinc deposition. An increase in the current density from 45 to 60 mA cm^{-2} and in electrolyte agitation from 60 to 412 rpm resulted in an increase in the cathodic potential and decrease in current efficiencies. A temperature increase from 35 to 45 °C led to a decrease in the cathodic potential. After a short initial electrodeposition (2–4 h) using a Pb–0.7%Ag anode, the lead content in the zinc deposit was higher than that obtained with a Pt anode (0.15 mg L^{-1} Pb^{2+}). A long deposition period of more than 72 h was also considered, and Pb content was almost the same in the zinc deposit for Pb^{2+} quantities (0.15 or 0.2 mg L^{-1}).
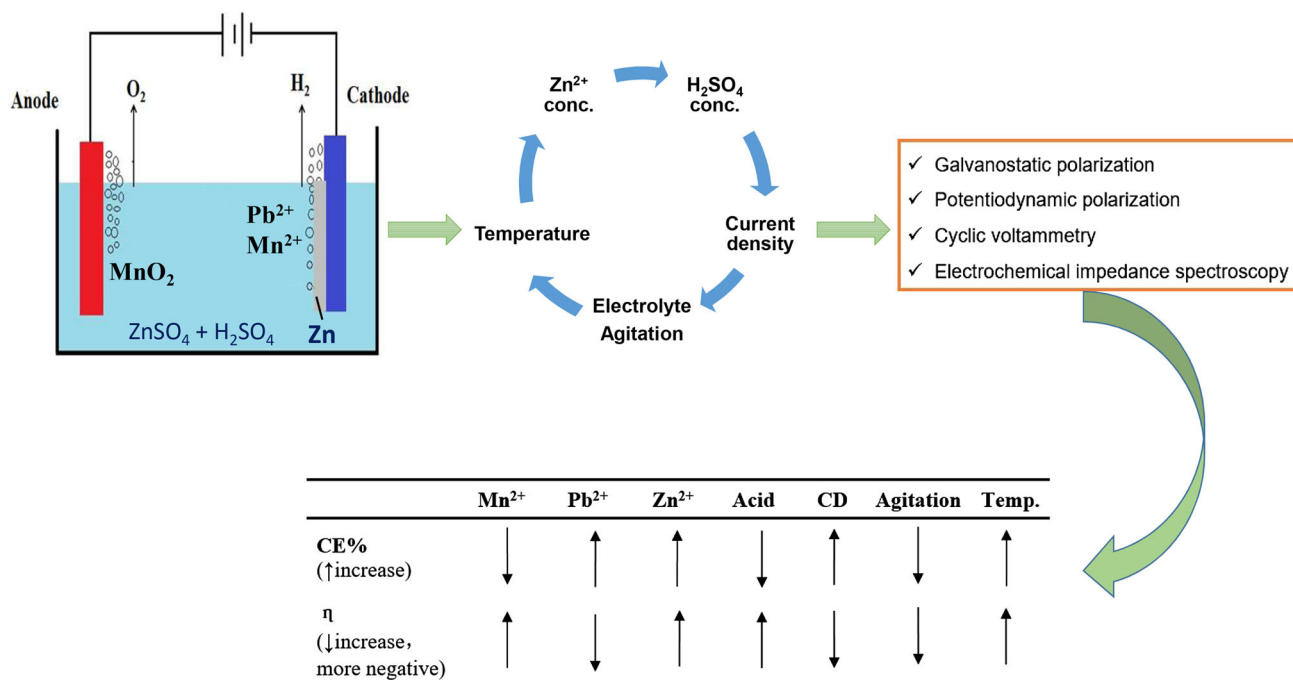
✉ C. Su
chaoran.su.1@ulaval.ca

1   Department of Mining, Metallurgical and Materials Engineering, Laval University, Québec City, QC G1V0A6, Canada

2   Hydro-Québec Research Centre (LTE), Shawinigan, QC G9N 7N5, Canada

Graphical Abstract

1 Introduction

The production of zinc from sulfides is predominantly conducted by a roast-leach-electrowinning process [1]. More than 80% of the power requirements of a zinc electrolytic refinery originate from the electrowinning process. It is important to operate the electrolysis as close as possible to the optimal operating conditions. Optimum electrolysis performance occurs when the specific energy consumption per ton of produced zinc is minimized. The two parameters that directly control energy consumption are current efficiency (CE) and total cell voltage [2]. The major variables affecting these two parameters are zinc and sulfuric acid concentrations, current density, temperature, metallic impurities, and additives [3]. The influence of electrolysis duration on deposition in the presence of impurities and additives is also a significant parameter to consider.

For zinc electrowinning, the overpotential of hydrogen evolution over zinc is very high in comparison with some other metals. The effect of impurities is an important consideration in the electrolysis process. Impurities in the electrolyte greatly affect the electrowinning process. Impurities that cause low hydrogen overpotential, such as antimony and nickel, result in a decrease in current efficiency [4, 5]. The negative role of lead as an impurity in

reducing the purity and quality of deposited zinc cannot be neglected as long as lead-based anodes are used in the zinc electrowinning process [3, 6].

In practice, the anodic potential corresponding to the applied current density could enable the formation of H_2O_2, which diffuses toward the cathode and has detrimental effects [7]. The dissolution of lead from the anode results in the formation of Pb^{2+} ions in solution, which are co-deposited at the cathode. Mansfeld and Gilman [8] showed that traces of lead on the cathode were beneficial, inhibiting dendritic growth of the zinc deposits. Mackinnon et al. [9] reported that the lead co-deposited with zinc causes an orientation change of the zinc crystals and increases cathodic polarization. As the original electrolyte contains manganese, other anodically formed species may also influence the cathodic process [10].

A strong correlation among polarization behavior, current efficiency, and morphology of zinc deposits has been shown by many research groups [3, 11–13]. Various impurities and additives can affect the polarization behavior of zinc deposition in a characteristic manner. It is possible to associate a given deposit morphology with a particular polarization (overpotential) condition [13]. Individual polarization and morphology observations or their combination may be used to obtain valuable information on the zinc electrodeposition process for potential applications to industrial plant practices and controls.

Scott et al. [14] found that higher cell temperatures reduced the energy consumption only in the presence of

additives capable of controlling deposit morphology. Bratt [15] provided a qualitative description of the major variables, such as impurities and additives, and considered them only for modeling. Fosnacht and O'Keefe [16] reported that increasing the acid concentration enhanced the hydrogen reduction on the cathode surface and increased zinc re-dissolution, leading to low current efficiency. Hosny et al. [17] provided limited industrial data on the effect of current density, with very little information for other variables.

The zinc deposit morphology and crystallographic orientation are extremely sensitive to lead levels as low as 1 mg L^{-1} in the electrolyte [9]. It is desirable to correlate the Pb content and the morphology of zinc deposits under chosen overpotentials and defined conditions of electrolysis. Manganese can decrease the negative effects of other impurities. Mn^{2+} is anodically oxidized to MnO_4^-. The latter immediately reacts with Mn^{2+} and produces Mn^{3+} and then MnO_2^- which can adsorb deleterious ions and affect the current efficiency of zinc deposition [10]. Hence, not only the impurity in the electrolyte but also the oxidized species produced at the anode characterize the behavior of zinc deposition.

The aim of this work is divided into two main objectives. The first is to study the effect of chemical composition of the electrolyte, such as the Mn^{2+}, Pb^{2+}, Zn^{2+}, and acid concentrations, on the zinc electrodeposition process and zinc deposit quality (Pb content and morphology). The second objective is to study the effect of operating parameters such as current density, temperature, and magnetic agitation on current efficiency, deposit morphology, cathodic polarization, and lead contamination.

2 Experimental

2.1 Reagents and electrolysis

The standard acidic zinc electrolyte was prepared from 60 g L^{-1} Zn^{2+} by adding $ZnSO_4 \cdot 7H_2O$ to 170 g L^{-1} H_2SO_4. The Mn^{2+} and Pb^{2+} cations were added as $MnSO_4 \cdot 2H_2O$ and $Pb(C_2H_3O_2)_2$, respectively. All reagents were supplied by Laboratories MAT and VWR Canada.

Laboratory-scale galvanostatic electrolysis was performed in 1000 mL of solution in a double-wall beaker thermostated at the desired working temperature. One plate of pure Al as the cathode and one plate of Pb–0.7wt.%Ag alloy or Pt as the anode were used. During the evaluation of the effect of Pb^{2+} ions in the electrolyte, a plate of Pt was also used as the anode. All electrode plates were mounted in polyester resin to obtain an exposed surface area of 1 cm^2. The reference electrode was Ag/AgCl/KCl$_{(sat)}$ (0.199 V vs SHE). The electrodes were mounted in a three-

cell electrode with an inter-distance of 2 cm. Before electrolysis, both the cathode and anode were manually polished using several grits of SiC paper, washed with distilled water and ethanol, and dried before immersion in the electrolyte. The three-cell electrode was connected to a potentiostat Gamry PC4/270-USA. All experiments were performed in duplicate ($\pm5\%$), and triplicate tests were also conducted when required.

2.2 Electrochemical measurements

Electrochemical studies were conducted employing cyclic voltammetry, potentiodynamic polarization, and electrochemical impedance techniques. Cyclic voltammetry (CV) experiments were performed with scanning from an initial potential of -1.3 V to a potential of -0.7 V at a scan rate of 10 mV s^{-1}. The potential was scanned from -1.05 to -1.25 V for the cathodic potentiodynamic polarization with a constant scan rate of 5 mV s^{-1}. The CV and potentiodynamic tests were performed using the potentiostat Gamry 3000-USA. The electrochemical impedance measurements were conducted using a Solartron 1255 HF frequency response analyzer and a Solartron 1286 electrochemical interface over the frequency range from 10 kHz to 0.5 Hz. The amplitude of the sinusoidal signal was maintained at 10 mV.

2.3 Deposit examination

The surface morphology and crystallographic orientation were determined using a scanning electron microscope (SEM, JEOL JSM-840a) and X-ray diffractometer (XRD, Siemens-D5000). The lead content in the deposit was measured using inductively coupled plasma (ICP, Optima 8300 ICP-OES).

3 Results and discussion

An initial galvanostatic duration of 2 h was considered for partial electrolysis (3.1) and zinc deposit characterization (3.2), whereas a long duration of galvanostatic polarization simulating industrial operating conditions is examined in Sect. 3.3.

3.1 Galvanostatic measurements

In the galvanostatic tests, a constant current was applied between the auxiliary and working electrodes. The potential of the working electrode was recorded versus time with respect to the reference electrode. The counter electrode was a Pb–0.7%Ag or Pt anode. After electrolysis, the deposit was rinsed, dried, and weighed for current

efficiency calculations using Faraday's law. The values of the cathodic potentials and current efficiencies are given in Table 1.
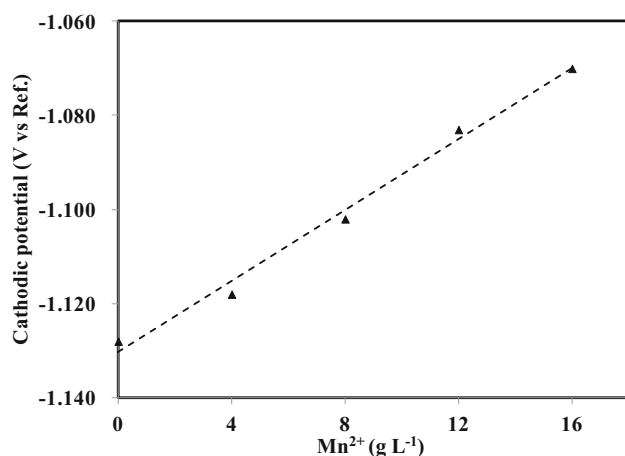
3.1.1 Effect of Mn²⁺ concentration

The profile of the cathodic potential was monitored for 2 h of electrodeposition in standard zinc electrolyte containing 170 g L⁻¹ H₂SO₄ and 60 g L⁻¹ Zn²⁺ at a current density of 52.5 mA cm⁻², 40 °C, and electrolyte agitation of 60 rpm. In this work, Pb–0.7%Ag was used as the anode. The influence of the Mn²⁺ ion concentration (0, 4, 8, 12, and 16 g L⁻¹) is shown in Fig. 1. Increasing the Mn²⁺ ion concentration in the zinc electrolyte decreased the overpotential of the zinc deposit. The measured cathodic potential without Mn²⁺ addition was −1.128 V and

Table 1 The cathodic potential and current efficiency values after 2 h of electrodeposition for Mn^{2+} and Pb^{2+} ion concentrations employing Pb–Ag or Pt anodes at various operating conditions

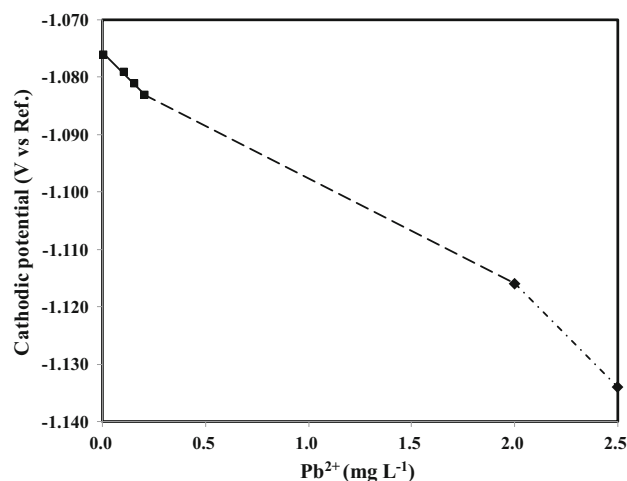| Parameters	Pb–Ag anode		Pt anode	
	CE (%)	Cathodic potential (V vs Ref.)	CE (%)	Cathodic Potential (V vs Ref.)
Mn^{2+} (g L⁻¹)				
0 (blank)	96.3	−1.128	12 g L⁻¹ Mn^{2+} was added with Pt anode for all experiments	
4	95.6	−1.118		
8	95.5	−1.102		
12	95.3	−1.083		
16	94.3	−1.072		
Pb^{2+} (mg L⁻¹)				
0 (blank)	Experiments with the Pb–Ag anode had no added Pb^{2+}		94.2	−1.076
0.1			94.4	−1.079
0.15			94.4	−1.081
0.2			94.7	−1.083
2			95.0	−1.116
2.5			95.6	−1.134
Zn^{2+} (g L⁻¹)				
56	94.6	−1.092	93.7	−1.088
60	95.3	−1.083	94.4	−1.081
65	95.5	−1.076	94.5	−1.075
H₂SO₄ (g L⁻¹)				
158	95.7	−1.096	95.5	−1.093
165	95.5	−1.090	95.0	−1.086
170	95.3	−1.083	94.4	−1.081
CD (mA cm⁻²)				
45	94.6	−1.072	93.8	−1.071
50	95.3	−1.081	94.1	−1.078
52.5	95.3	−1.083	94.4	−1.081
60	95.9	−1.089	95.5	−1.088
Agitation (rpm)				
60	95.3	−1.083	94.4	−1.081
100	95.1	−1.090	93.8	−1.088
412	94.7	−1.093	93.6	−1.090
Temperature (°C)				
35	95.1	−1.096	94.1	−1.093
38	95.2	−1.081	94.2	−1.0825
40	95.3	−1.083	94.4	−1.081
45	95.9	−1.074	95.1	−1.073

Fig. 1 Effect of Mn^{2+} ion concentrations on the cathodic potential employing a Pb–0.7%Ag anode on the zinc deposit in electrolyte containing 170 g L^{-1} H_2SO_4 and 60 g L^{-1} Zn^{2+} at a current density of 52.5 mA cm^{-2}, 40 °C and agitation of 60 rpm

Fig. 2 Effect of Pb^{2+} ion concentrations on the cathodic potential of the Zn deposit employing a Pt anode in electrolyte containing 170 g L^{-1} H_2SO_4, 60 g L^{-1} Zn^{2+}, and 12 g L^{-1} Mn^{2+} at a current density of 52.5 mA cm^{-2}, 40 °C, and agitation of 60 rpm

gradually decreased to less negative values with the addition of Mn^{2+} up to −1.072 V at 16 g L^{-1} (Table 1). This depolarization of 56 mV might be due to the effect of MnO_4^- formation at high concentrations of Mn^{2+}, which catalyzes the hydrogen evolution reaction (HER) and reduces its overpotential [10].

Although manganese in the electrolyte is beneficial in enhancing the anodic reaction and reducing lead-base anode corrosion [18, 19], its negative effect on the cathodic current efficiency cannot be neglected. The effect of Mn^{2+} concentrations on the CE% was examined for Pb–Ag anodes (Table 1). The current efficiency values were decreased by 0.75, 0.81, 0.99, and 2.04% with the addition of 4, 8, 12, and 16 g L^{-1} Mn^{2+}, respectively. The decrease in CE% was relatively low at concentrations from 4 to 12 g L^{-1}, with a sharp decrease at the higher concentration of 16 g L^{-1}. Increasing the concentration of Mn^{2+} in the electrolyte (up to 16 g L^{-1}) decreased the CE% by almost 2%. A concentration of 12 g L^{-1} of manganese, which corresponds to 95.3% CE, was considered for all subsequent tests. The decrease in CE% could also be attributable to the catalytic effect of MnO_4^- ions on the HER, which also causes a decrease in Zn^{2+} reduction as mentioned by Zhang and Hua [10].

3.1.2 Effect of Pb^{2+} concentration

The effect of 0, 0.1, 0.15, 0.2, 2, and 2.5 mg L^{-1} Pb^{2+} ions when added to the standard zinc sulfate electrolyte containing 12 g L^{-1} Mn^{2+} on the cathodic potential is shown in Fig. 2. During these experiments, Pt was used as the anode to study the effect of Pb^{2+} ions alone without the effect of dissolution of the Pb–Ag anode. As shown in Fig. 2, the addition of lead to the electrolyte increased the

cathodic potential. This potential was −1.076 V in the absence of lead ions. The observed increase in the zinc deposition overpotential (more negative) was more for the initial low quantities of lead ions up to a concentration of 0.2 mg L^{-1}. This value increased slowly by a few millivolts with the addition of Pb^{2+} (−1.083 V), reaching −1.134 V at the maximum addition of 2.5 mg L^{-1} Pb^{2+} (Table 1). This could be due at least partially to the increase in hydrogen overpotential on the deposited lead surface.

As shown in Table 1, lead addition increased the CE%. During the 2 h of electrodeposition, the current efficiencies increased from 94.2 to 94.7% with the addition of 0.2 mg L^{-1} Pb^{2+}. The maximum addition of 25 g L^{-1} Pb^{2+} increased the CE% up to 95.6%. The effect of a long duration of electrodeposition in the presence of Pb^{2+} is discussed in Sect. 3.3.

3.1.3 Effect of Zn^{2+} concentration

Figure 3 shows the evolution of the cathodic potential during zinc electrodeposition in an electrolyte containing different concentrations of zinc (56, 60, and 65 g L^{-1} of Zn^{2+}). In this series of experiments, Pb–0.7%Ag or Pt was used as the anode. The increase in Zn^{2+} ions in the zinc electrolyte decreased the overpotential of zinc electrodeposition for both anodes (Fig. 3). However, the overpotentials were slightly higher with the Pb–0.7%Ag anode than with the Pt anode due to the higher Pb^{2+} ion concentration with the Pb–0.7%Ag anode during the initial 2 h of electrolysis.

Increasing the Zn^{2+} concentration from 56 to 60 g L^{-1} increased the CE% by 0.7% (from 94.6 to 95.3%) using
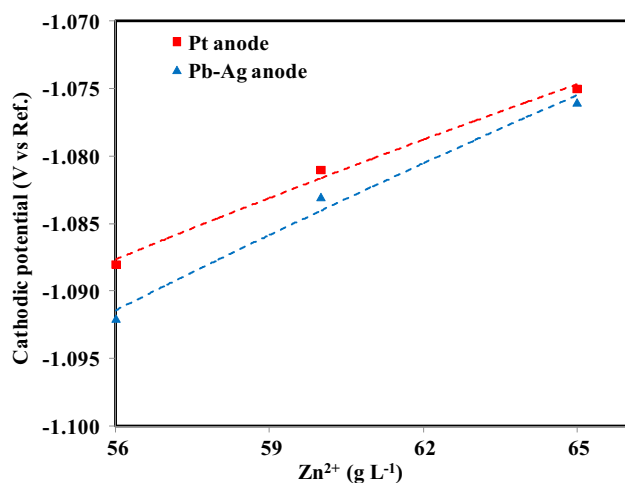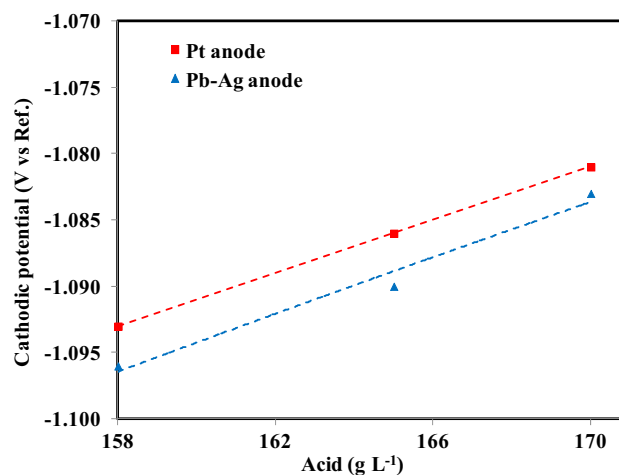
Fig. 3 Effect of different zinc contents on the cathodic potential during Zn electrowinning employing a Pb–0.7%Ag anode (■) or Pt anode (▲) with the addition of 0.15 mg Pb^{2+} impurity into zinc electrolyte containing 170 g L^{-1} H_2SO_4 and Mn^{2+} 12 g L^{-1} at a current density of 52.5 mA cm^{-2}, 40 °C, and agitation of 60 rpm
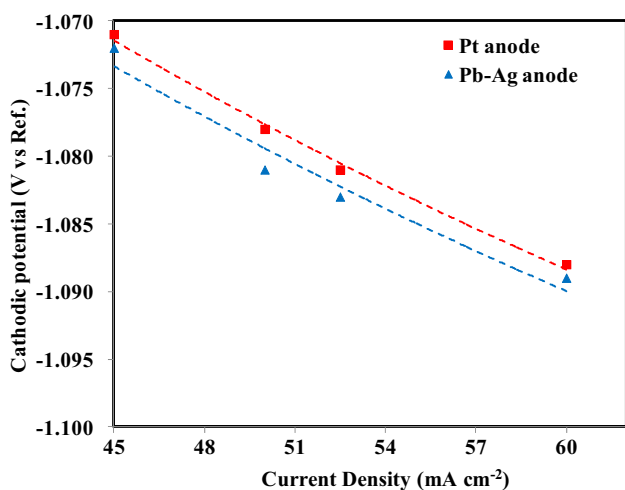

Fig. 4 Effect of different sulfuric acid concentrations on the cathodic potential during Zn electrowinning employing a Pb–0.7%Ag anode (■) or Pt anode (▲) with the addition of 0.15 mg Pb^{2+} impurity in zinc electrolyte containing 60 g L^{-1} Zne and 12 g L^{-1} Mn^{2+}, at a current density of 52.5 mA cm^{-2}, 40 °C, and agitation of 60 rpm

Pb–0.7%Ag as the anode. However, only a 0.2% increase in CE% was obtained with a further increase in Zn^{2+} ion up to 65 g L^{-1}. The calculated current efficiencies after electrolysis using the Pt anode exhibited the same trend (Table 1). Thus, at higher concentrations (>60 g L^{-1} Zn^{2+}), the current efficiency is slightly improved by increasing the Zn^{2+} ions in the electrolyte. Increasing the Zn^{2+} concentration increased the difficulty of Pb^{2+} co-deposition, decreasing the beneficial effect of lead on the cathodic potential and current efficiency. This is observed mainly for the range of concentration of zinc from 56 to 60 g L^{-1} region, than that of 60–65 g L^{-1} for both cathodic overpotential and CE. This behavior could be related to the solution viscosity and the availability of active sites on the limited surface. With the Pt anode, the CE was lower by ∼1% for all zinc concentrations compared to the Pb–0.7%Ag anode. The effect of Mn^{2+} on the cathodic reaction was stronger with the Pt anode due to cathodic depolarization by MnO_4^{-}, since part of the added Mn was already consumed as a protective layer for the Pb–0.7%Ag anode.

3.1.4 Effect of H_2SO_4 concentration

As shown in Fig. 4, the overpotential of the zinc deposit was decreased by 17 mV (for the Pb–0.7%Ag) and 11 mV (for the Pt anode) as the sulfuric acid concentration increased from 158 to 170 g L^{-1}. Increasing the sulfuric acid in the zinc electrolyte accelerated the HER reaction due to the increase in H^+ cations in the double layer. This depolarization was accompanied by a reduction in the

current efficiencies (Table 1). Considering the lead-base anode during electrolysis, the CE% decreased from 95.7 to 95.3% as the acid content increased from 158 to 170 g L^{-1}, and the reduction of CE% was more significant in the case of Pt as the anode, very probably due to the simple reduction of added protons onto the cathode. At such low potential, high evolution of hydrogen gas at the cathode could increase electrolyte agitation and hydrogen ion diffusion and retard the Zn^{2+} reduction process.

3.1.5 Effect of current density

Figure 5 shows that when the current density (CD) increased from 45 to 60 mA cm^{-2}, the cathodic potential increased from −1.072 to −1.089 mV using the Pb–0.7%Ag anode. The potential of the zinc deposit was more negative for the Pb–0.7%Ag anode than for the Pt anode under the same operating conditions. During zinc electrowinning, the concentration of Pb^{2+} ions dissolved in the zinc electrolyte employing the Pb–0.7%Ag anode at higher current densities was more than that with the Pt anode, which increased the overpotential of zinc electrodeposition (Table 1).

A remarkable influence of the current density on the cathodic CE was observed. For instance, increasing the CD from 45 to 60 mA cm^{-2} led to an increase in CE% from 94.6 to 95.9% in the case of the Pb–0.7%Ag anode. A similar trend of increasing current efficiency was also obtained in the case of the Pt anode. The hydrogen overvoltage increased at high current densities, resulting in higher CE and favoring Zn^{2+} reduction.

Fig. 5 Effect of current density on the cathodic potential during Zn electrowinning employing a Pb–0.7%Ag anode (■) or Pt anode (▲) with the addition of 0.15 mg Pb^{2+} impurity in the electrolyte containing 170 g L^{-1} H_2SO_4, 60 g L^{-1} Zn^{2+}, and 12 g L^{-1} Mn^{2+} at 40 °C and agitation of 60 rpm

3.1.6 Effect of the electrolyte agitation rate

The effect of agitation rates on the cathodic polarization is shown in Fig. 6. Increasing the electrolyte agitation rate from 60 to 100 rpm led to an increase in the cathodic potential of 7 mV for either anode (Pb–0.7%Ag or Pt anodes). This higher agitation rate increased the overpotential of the Zn^{2+} reduction rate and favored the hydrogen parasitic reaction. At speeds higher than 100 rpm up to 412 rpm, the cathodic potentials were almost stable. The
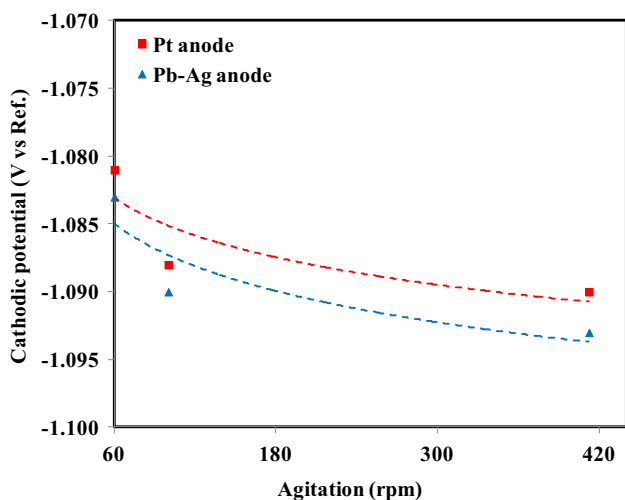
current efficiency decreased by 0.2 and 0.6% at 100 and 412 rpm compared to 60 rpm (Table 1). This could be due to the relative increase in the diffusion and reduction rates of hydrogen ions compared to zinc ions. Increasing the agitation speed in this range had a negative influence on zinc electrowinning, showing more cathodic polarization and lower current efficiency.

3.1.7 Effect of temperature

Increasing the electrolyte temperature from 35 to 45 °C led to a decrease of 22 mV in the overpotential of the zinc deposition (Pb–0.7%Ag anode). The increase in temperature had a positive effect by decreasing energy consumption during zinc electrowinning. In addition, the cathodic current efficiency increased at higher temperatures (Table 1). This increase could be linked to an increase in the diffusion rate of zinc ions in the electrolyte bath due to a decrease in electrolyte viscosity and the enhancement of the reduction reaction rate of zinc ions at the cathode surface to produce zinc metal ($Zn^{2+} + 2e^- \rightarrow Zn_{(s)}$). Also, the electrolyte conductivity increases with temperature, which decreases the cell voltage and the required energy.

The presence of lead ions in the zinc electrolyte at different temperatures decreased the overpotential of the zinc deposition (Fig. 7). Both anodes showed the same tendency; however, more negative values were observed in the case of the Pb–0.7%Ag anode. The influence of temperature could be a function of several variable factors, such as depolarization, the diffusion rate, and lead ion content. The
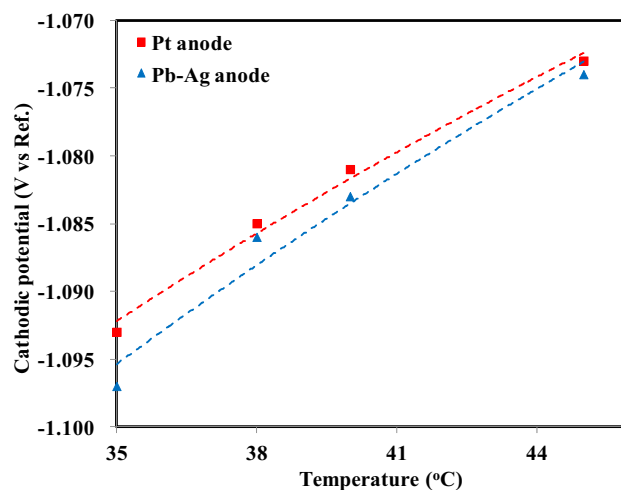

Fig. 6 Effect of agitation rate on the cathodic potential during Zn electrowinning employing a Pb–0.7%Ag anode (■) or Pt anode (▲) and addition of 0.15 mg Pb^{2+} as an impurity in zinc electrolyte containing 170 g L^{-1} H_2SO_4, 60 g L^{-1} Zn^{2+}, and 12 g L^{-1} Mn^{2+} at current density of 52.5 mA cm^{-2} and 40 °C

Fig. 7 Effect of temperature on cathodic potential during Zn electrowinning employing a Pb–0.7%Ag anode (■) or Pt anode (▲) with the addition of 0.15 mg Pb^{2+} impurity in zinc electrolyte containing 170 g L^{-1} H_2SO_4, 60 g L^{-1} Zn^{2+}, 12 g L^{-1} Mn^{2+}, and 0.15 mg Pb^{2+} as an impurity at a current density of 52.5 mA cm^{-2} and agitation at 60 rpm

CE values increased with increasing temperature regardless of the anode employed. For example, in the case of the Pb–0.7%Ag anode, the CE was 95.1% at 35 °C and increased up to 95.9% at 45 °C. This increase could reflect a smaller influence on the hydrogen reduction reaction than Zn deposition and the increased dissolution of lead ions in solution at higher temperatures.

The effects of Mn^{2+}, Pb^{2+}, and different operating parameters on CE% and cathodic potential in zinc electrowinning process are summarized in Table 2. The CE% was increased by increasing Pb^{2+} and Zn^{2+} ion concentrations in the electrolyte as well as by increasing the operating temperature. Cathodic depolarization was observed by increasing the concentrations of Mn^{2+} and Zn^{2+}, acidity, and the temperature of the electrolyte. The cathodic overpotentials increased with increasing lead ion concentrations and obviously increased with current density.

3.2 Deposit examination

The obtained zinc deposits were examined using SEM and XRD to determine surface morphology and crystallographic orientations, respectively. SEM photomicrographs are shown in Fig. 8. The crystallographic orientations and the lead contamination determined by ICP of the zinc deposits from the zinc electrolyte containing Pb^{2+} and Mn^{2+} ions employing different parameters are given in Table 3.

These findings have revealed that the crystallographic orientation obtained from the standard electrolyte without manganese addition was (101) (102) (103), and the predominant orientation (101) was not affected by the addition of Mn^{2+} ions when employing the Pb–0.7%Ag anode. A compact smooth deposit with medium grain size was obtained at higher concentrations of Mn^{2+} (Fig. 8b). The lead content in the deposit decreased from 5.23 (in the

absence of Mn^{2+}) to 1.36 ppm with Mn^{2+} addition at 16 g L^{-1}. This finding confirms the important beneficial effect of Mn^{2+} addition for forming a protective MnO_2 layer on the lead-based anode, leading to less soluble lead in the electrolyte.

The addition of low concentrations (0.1–0.2 mg L^{-1}) of Pb^{2+} ions resulted in an orientation of the deposit similar to that of the standard (101) (102) (103) (Fig. 8c). As the lead concentration was increased up to 2 mg L^{-1}, the deposit became slightly more compact with a completely different orientation (103), compared to the previous predominant one (Fig. 8d). The addition of a high concentration of Pb^{2+} (2.5 mg L^{-1}) led to an orientation of (002) (103) (101). Thus, a high concentration of lead in the electrolyte negatively affects the crystallographic orientation and surface morphology. The addition of soluble lead in the electrolyte generally increased the lead contamination in the zinc deposit, and the highest Pb^{2+} ion addition increased the lead content up to 12.70 ppm. This co-deposition also resulted in a change in morphology.

The increase in zinc ions in the electrolyte had no effect on either morphology or crystallographic orientation but reduced the contamination of the deposit by lead: the content of lead decreased from 1.67 to 1.17 ppm with the addition of 65 g L^{-1} compared to 56 g L^{-1} Zn^{2+} with the lead-base anode (Table 3). A similar trend was obtained with the Pt anode. The studied range of sulfuric acid concentrations (158–170 g L^{-1}) did influence the main crystallographic orientation (101), and at high concentrations, the platelet size of the deposit was larger than that at low concentrations (Fig. 8e, f). As shown in Table 3, the lead contamination was reduced by employing both anodes at high acid content; this could be due to the relative H$^+$ diffusion and the acceleration of the HER.

At low current density (45 mA cm^{-2}), the morphology of deposit showed large crystals although the orientation did not change (Fig. 8g). Increasing the current density up

Table 2 Trends of current efficiency (CE%) and overpotential (η) as a function of increasing various operating conditions and parameters of the cathodic potential

	Mn^{2+}	Pb^{2+}	Zn^{2+}	Acid	CD	Agitation	Temp.
CE% ↑increase	↓	↑	↑	↓	↑	↓	↑
H ↓increase (more negative)	↑	↓	↑	↑	↓	↓	↑
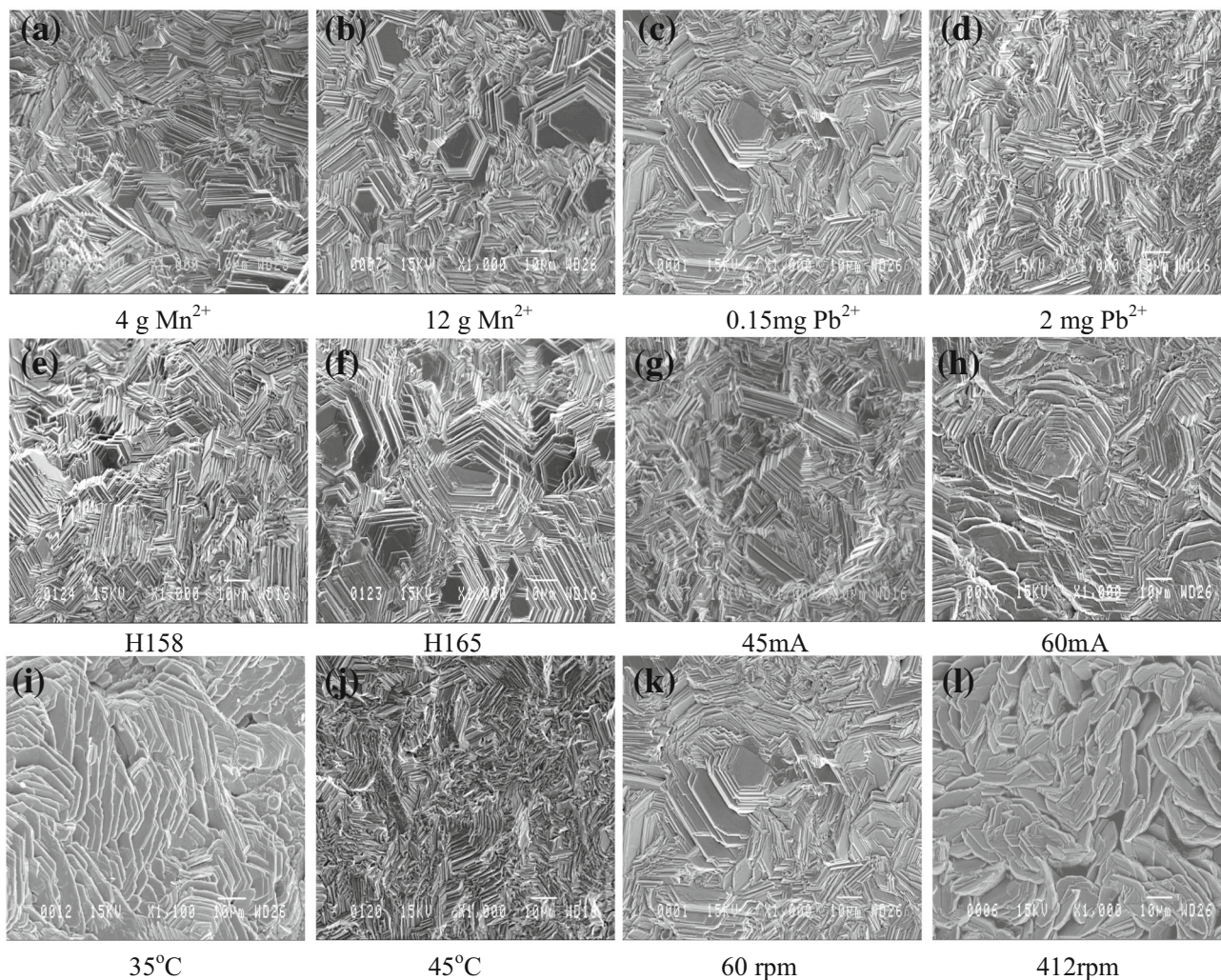
Fig. 8 Scanning electron microscopy photomicrographs (×1000) of the zinc deposit in the presence of Mn^{2+} and Pb^{2+} ions employing the different parameters described in Table 3 for the different anodes (**a**, **b**, **e**, **f**, **i**, **j** for the Pb anode and **c**, **d**, **g**, **h**, **k**, **l** for the Pt anode)

to 60 mA cm^{-2} improved the grain size (Fig. 8h) and was accompanied by an increase in overpotential, which led to more zinc contamination by lead (Table 3). Thus, the current density is a critical parameter that also influences the morphology.

The agitation rate did not influence the morphology or the orientation of the deposit but resulted in an increase in lead contamination in the zinc deposit. At a low agitation rate (60 rpm), the lead content in the deposit was 1.40 and 1.35 ppm with the Pb–0.7%Ag and Pt anodes, respectively. The contamination increased to 1.71 and 1.69 ppm at the highest speed (412 rpm) with the two anodes, respectively (Table 3).

At low temperature (35 °C), the crystallographic orientation changed to (002) (103) (101), giving a random needled deposit (Fig. 8i). Increasing the temperature restored the standard orientation of the zinc deposit. The

lead content in the deposit decreased as the temperature increased. Thus, temperature is an important factor in grain refining, and the optimal working temperature is 38–40 °C.

3.3 Long duration galvanostatic tests

3.3.1 Cathodic potential

Electrolysis tests over a period of 72 h were conducted to examine the effect of Pb^{2+} ions and the lead-base anode on zinc deposit contamination. The effect of Pb impurity on the cathodic potentials during different electrolysis durations of 1, 2, 4, 24, 48, and 72 h was evaluated by galvanostatic measurements at 52.5 mA cm^{-2} employing a Pb–0.7%Ag or Pt anode. The zinc electrolyte contained 12 g L^{-1} Mn^{2+} at 40 °C, and two different concentrations of Pb^{2+} ions, 0.15 and 0.2 mg L^{-1}, were added to the zinc

Table 3 Crystallographic orientation and lead content in the zinc deposits in the presence of Mn^{2+} and Pb^{2+} ions utilizing different working parameters

Parameters	Pb–0.7%Ag anode		Pt anode	
	Crystallographic orientation (hkl)	Pb cont. (ppm)	Crystallographic orientation (hkl)	Pb cont. (ppm)
Mn^{2+} (g L^{-1})				
0	(101) (102) (103)	5.23	12 g L^{-1} Mn^{2+} was added with Pt anode for all experiments	
4	(101) (102) (103)	2.89		
8	(101) (102) (103)	1.57		
12	(101) (103) (102)	1.40		
16	(101) (103) (102)	1.36		
Pb^{2+} (mg L^{-1})				
0	Experiments with the Pb–Ag anode had no added Pb^{2+}		(101) (102) (103)	–
0.1			(101) (102) (103)	1.13
0.15			(101) (102) (103)	1.35
0.2			(101) (103) (102)	1.46
2			(103) (101) (102)	8.94
2.5			(002) (103) (101)	12.70
Zn^{2+} (g L^{-1})				
56	(101) (103) (102)	1.67	(101) (102) (103)	1.65
60	(101) (103) (102)	1.40	(101) (102) (103)	1.35
65	(103) (101) (102)	1.17	(103) (101) (102)	1.21
H_2SO_4 (g L^{-1})				
158	(101) (103) (102)	1.59	(101) (103) (102)	1.50
165	(101) (102) (103)	1.44	(101) (103) (102)	1.41
170	(101) (103) (102)	1.40	(101) (102) (103)	1.35
CD (mA cm^{-2})				
45	(101) (103) (102)	1.29	(101) (102) (103)	1.19
50	(101) (103) (102)	1.37	(101) (102) (103)	1.29
52.5	(101) (103) (102)	1.40	(101) (102) (103)	1.35
60	(101) (102) (103)	1.45	(101) (102) (103)	1.44
Agitation (rpm)				
60	(101) (103) (102)	1.40	(101) (102) (103)	1.35
100	(101) (102) (103)	1.67	(101) (102) (103)	1.64
412	(101) (103) (102)	1.71	(101) (103) (102)	1.69
Temperature (°C)				
35	(002) (103) (101)	1.62	(103) (101) (102)	1.58
38	(101) (103) (102)	1.46	(101) (102) (103)	1.43
40	(101) (103) (102)	1.40	(101) (102) (103)	1.35
45	(101) (103) (102)	1.28	(101) (102) (103)	1.22

electrolyte with the Pt anode, whereas no Pb^{2+} ions were added to the zinc electrolyte when the Pb–0.7%Ag anode was used. The results are shown in Fig. 9.

As shown in Fig. 9, the three curves are close with similar tendencies. During the initial 10 h, the potential shifted to less negative values (possibly due to lead deposition) and then shifted slowly to less negative potentials during 10–24 h. After 24 h, the potential was less negative at 0.2 mg L^{-1} than for the Pb–0.7%Ag anode, reaching a plateau that was maintained until the end of the 72 h of deposition. In the zinc electrolyte containing 0.15 mg L^{-1} Pb^{2+}, the cathodic potential was −1.047 V, whereas the polarization increased to −1.050 V when the lead ion concentration was increased to 0.2 mg L^{-1}. When Pb–0.7%Ag was used as the anode, the cathodic potential of the zinc deposit without external addition of Pb^{2+} ions was

Fig. 9 Cathodic polarization curves of the zinc deposit at 52.5 mA cm^{-2} and 40 °C in zinc electrolyte containing 170 g L^{-1} H$_2$SO$_4$, 60 g L^{-1} Zn^{2+}, and 12 g L^{-1} Mn^{2+} with the Pb–0.7%Ag anode and two different Pb additions with the Pt anodes at different times of electrolysis
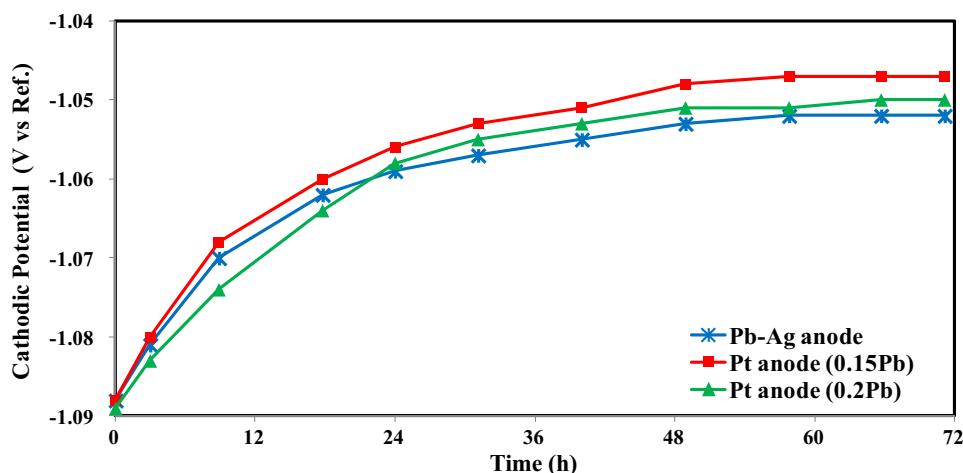
Table 4 Lead content in the zinc deposit and electrolyte after different electrolysis times of 1, 2, 4, 24, 48, and 72 h in the standard zinc electrolyte containing 170 g L^{-1} H$_2$SO$_4$, 60 g L^{-1} Zn^{2+}, 12 g L^{-1} Mn^{2+}, and various lead ion concentrations using the Pb–Ag or Pt anode at 52.5 mA cm^{-2}, 40 °C, and agitation of 60 rpm

Time (h)	Lead content (ppm)					
	Pb–Ag anode		Pt anode (0.15 mg L^{-1} Pb^{2+})		Pt anode (0.2 mg L^{-1} Pb^{2+})	
	Electrolyte	Deposit	Electrolyte	Deposit	Electrolyte	Deposit
1	0.92	1.38	0.88	1.34	0.96	1.45
2	0.74	1.40	0.85	1.35	0.95	1.46
4	0.66	1.44	0.83	1.38	0.93	1.48
24	0.69	1.66	0.71	1.47	0.88	1.57
48	0.63	1.73	0.46	1.65	0.64	1.70
72	0.74	1.98	0.17	1.90	0.25	1.94

more negative than the other two curves with Pt but showed the same tendency. The cathodic potential was −1.088 V after the first hour and reached −1.052 V after 50 h, becoming stable at 50–72 h. This profile reflects the higher corrosion rate of the lead-base anode during the initial few hours. The quantity of soluble lead obtained from anode corrosion was less than 0.15–0.2 mg L^{-1}, especially during the first few hours. The nucleation of zinc germs requires more energy than grain size growth [20]. The zinc reduction becomes relatively easier with time as the first layer of zinc is formed and zinc is subsequently deposited on zinc rather than on the aluminum substrate.

### 3.3.2 Lead content in the deposit and electrolyte

The Pb content in the zinc deposit and in the zinc electrolyte was analyzed using ICP. The results are shown in Table 4 and Fig. 10.

Figure 10a shows that when platinum was used as the anode, the addition of 0.2 mg L^{-1} Pb^{2+} resulted in more Pb content in the zinc deposit compared to the addition of

0.15 mg L^{-1}, and lead contamination slightly increased with time. Employing the Pb–0.7%Ag anode from 1 to 72 h resulted in a large increase in contamination (1.38–1.98 ppm) (Table 4).

At the end of 2 h of electrowinning, the Pb content in the zinc deposit employing the Pb–0.7%Ag anode was more than that of the Pt anode with the addition of 0.15 mg L^{-1} Pb^{2+} and lower than that of the Pt anode with the addition of 0.2 mg L^{-1} Pb^{2+}. However, at the end of 72 h of electrowinning, the Pb content in the zinc deposit using the Pb–0.7%Ag anode (1.98 ppm) was almost the same as that with Pt anodes (1.90 and 1.94 ppm for the addition of 0.15–0.2 mg L^{-1} Pb^{2+}, respectively). Thus, the lead contamination originating from the lead anode was nearly between 0.15 and 0.2 mg L^{-1}.

Figure 10b shows the evolution of the Pb content in the electrolyte as a function of time for the Pb–0.7%Ag anode and for two different quantities of added lead ions with the Pt anode. These results can provide a better understanding of the remaining non-deposited Pb^{2+} in the electrolyte.

(a)

(b)
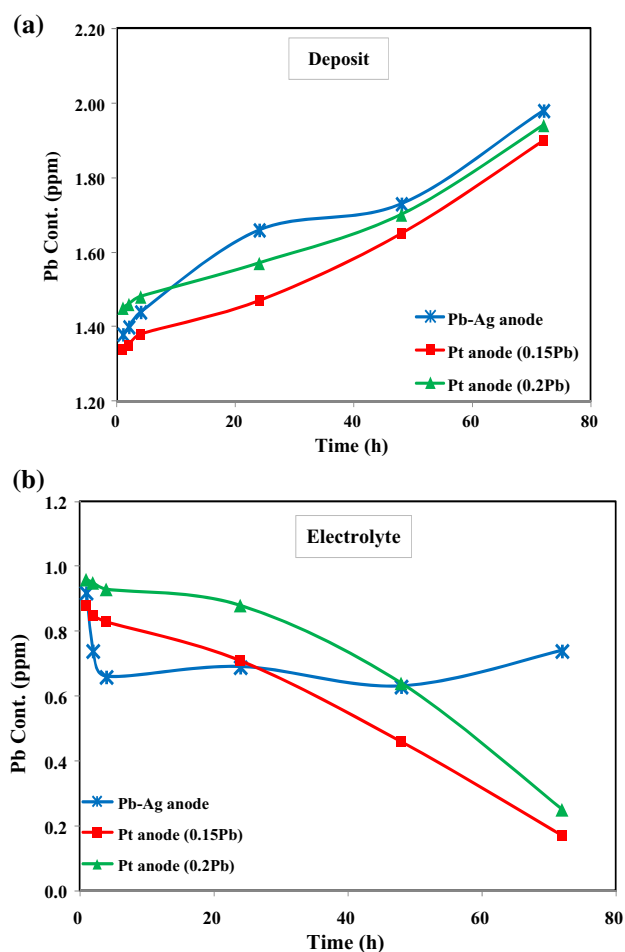
Fig. 10 Pb contamination in the **a** zinc deposit and **b** zinc electrolyte containing 170 g L^{-1} H_2SO_4, 60 g L^{-1} Zn^{2+}, and 12 g L^{-1} Mn^{2+} at 52.5 mA cm^{-2}, 40 °C and agitation of 60 rpm with the Pb–0.7%Ag anode and Pt anode at different Pb additions (0.15 and 0.2 mg L^{-1}) during different electrolysis time periods of 1, 2, 4, 24, 48, and 72 h

During the first hour, the electrolyte with the Pb–0.7%Ag anode had more lead than that after 2 h because the protection of the anode by the MnO_2 layer was not complete. A steady value of the lead content in the electrolyte was observed (approximately 0.7 ppm) after 8 h up to 72 h, revealing an equilibrium between lead dissolution from the anode covered by the MnO_2 layer and the Pb^{2+} deposition rate. In the case of external addition of lead with the Pt anode, the remaining lead in the examined two

electrolytes decreased to 26–29% during the last 48 h. This decrease could be due to a less negative electrodeposition potential which favored lead deposition and a very sensitive decrease in lead ions in the electrolyte.

3.3.3 Current efficiency

The calculated current efficiency values during 72 h of electrodeposition are given in Table 5. The CE% decreased with increasing electrodeposition time. In the case of the Pb–0.7%Ag anode, the CE after 2 h was 95.3% and decreased to 92.8% after 24 h and 89.5% after 72 h. This decrease could be partially explained by the decrease in the lead quantity in the electrolyte from approximately 0.92 to an average of 0.70 ppm and the effect of this impurity on the incubation time and current efficiency in zinc electrowinning [21].

The same trend was observed when the platinum anode was employed with the addition of soluble lead ions to the electrolyte at the beginning. The initial CE was 94.4–94.5% after adding 0.15–0.2 mg L^{-1} Pb^{2+} ions, respectively. After 72 h, the CE decreased to 87.2–88.5%. This sharp drop in CE values with a long duration of galvanostatic polarization can be explained by the reduced effect of the soluble lead at lower concentrations. Non-adherent deposits and re-dissolution of the zinc deposit into the electrolyte could also be considered.

3.4 Electrochemical measurements

Electrochemical measurements based on potentiodynamic polarization, cyclic voltammetry, and electrochemical impedance spectroscopy were conducted for zinc deposition under atmospheric conditions to study the effect of different temperatures (35, 38, 40, 45 °C) and concentrations of sulfuric acid and zinc sulfate with 0.15 mg L^{-1} Pb^{2+} ions.

3.4.1 Potentiodynamic polarization

Important information about the kinetic parameters, such as the cathodic Tafel slope and overpotential of zinc reduction, can be obtained using potentiodynamic polarization.

Table 5 Current efficiency values after different electrolysis times of 2, 4, 24, 48, and 72 h

Time (h)	Current efficiency (%)		
	Pb–0.7%Ag anode	Pt anode (0.15 mg L^{-1} Pb^{2+})	Pt anode (0.2 mg L^{-1} Pb^{2+})
2	95.3	94.5	94.4
4	95.1	94.3	94.1
24	92.8	92.5	92.4
48	91.4	91.1	90.7
72	89.5	88.5	87.2

During polarization from -1.35 to -1.05 V at a scan rate of 5 mV s^{-1}, the theoretical cathodic overpotential is calculated as follows:

$$E_{e,Zn} = -0.763 + (RT/2F)\ln[a_{Zn^{2+}}/a_{Zn}]$$

$$E_{e,H_2} = 0.0 + (RT/F)\ln\left[a_{H^+}/\left(a_{H_2}\right)^{0.5}\right]$$

$$\eta_{Zn} = E_m - (E_{e,Zn} + E_{e,H_2}),$$

where E_e is the equilibrium potential, R is the gas constant, T is the working temperature in K, F is Faraday's constant (equal to 96,500 C mol^{-1}), and E_m is the measured potential at a specific current density (52.5 mA cm^{-2}) [22].

The cathodic Tafel slope was determined by extrapolating two selected points on the cathodic curve of log I-E; the first point was $\sim$50–100 mV from the corrosion potential, and the other point was further far by one decade of the current density [23]. The results are shown in Table 6.

Figure 11 shows the effect of different concentrations of zinc ions on the cathodic behavior. Increasing the zinc ion concentration from 56 to 65 g L^{-1} in the presence of manganese alone decreased the cathodic overpotential from 117 to 107 mV, respectively. The same decreasing trend was obtained by combining manganese with 0.15 mg L^{-1} Pb^{2+} ions. For all cases, the Tafel slope values were increased slightly by increasing the zinc concentration. However, the values of cathodic Tafel slope were between 114 an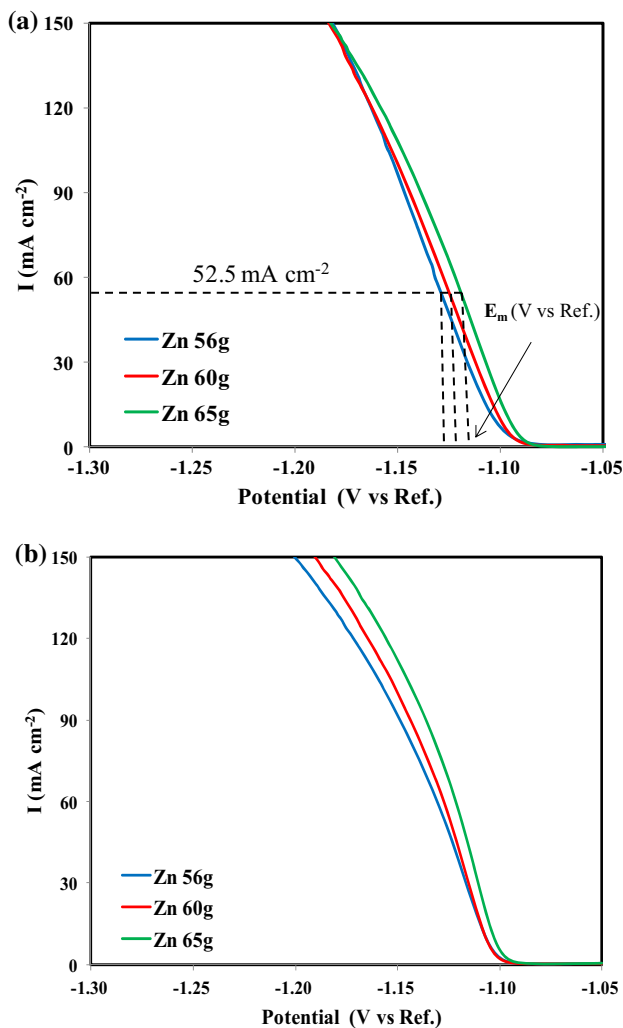d 122 mV decade^{-1}. This indicates that there were no changes in the mechanisms of the hydrogen [24] and zinc reduction reactions.

The effect of sulfuric acid concentration on zinc reduction is shown in Fig. 12. Increasing the concentration of acid significantly decreased the cathodic overpotential in the presence and absence of lead. In the absence of lead, the η value decreased from 136 to 113 mV as the acid concentration increased from 158 to 170 g L^{-1}, respectively. This decrease in overpotential was much more pronounced in the presence of lead, with a decrease from 153 to 114 mV at the same acid concentrations. Increasing the acid content in the electrolyte resulted in a higher H$^+$ ion concentration in solution which increased hydrogen evolution and reduced zinc reduction. The addition of lead (0.15 mg L^{-1}) to the zinc electrolyte also resulted in higher overpotential due to the co-deposition of lead with zinc. The value of b_c was also decreased by increasing the acid concentration but remained within the range of 115 to 123 mV decade^{-1} (Table 6).

Increasing the temperature resulted in a decrease in the overpotential due to the decrease in viscosity and high movement of ions in the electrolyte at high temperature. These changes result in an increase in cations moving toward the cathode, which obtain more electrons and decrease the cathodic potential. The increase in the agitation rate from 60 to 412 rpm increased the overpotential from 113 to 120 mV, respectively, confirming the galvanostatic results. It is significant that this parameter

Table 6 The cathodic overpotential and Tafel slope values at different working parameters with the Pt anode

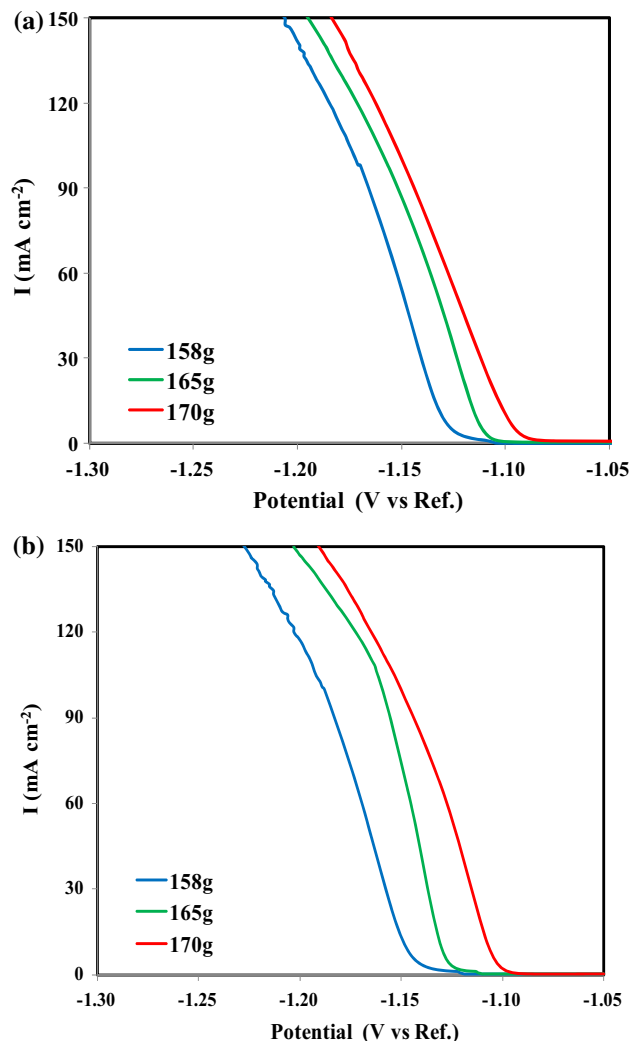| Parameters	12 g L^{-1} Mn^{2+}		12 g L^{-1} Mn^{2+} and 0.15 g L^{-1} Pb^{2+}	
	$-\eta_{(52.5)}$ (mV vs SHE)	Tafel slope $(-b_c)$ (mV decade^{-1})	$-\eta_{(52.5)}$ (mV vs SHE)	Tafel slope $(-b_c)$ (mV decade^{-1})
Zn^{2+} (g L^{-1})				
56	117	119	116	122
60	113	115	114	119
65	107	114	108	117
H$_2$SO$_4$ (g L^{-1})				
158	136	123	153	123
165	120	117	130	122
170	113	115	114	119
Agitation (rpm)				
60	113	115	114	119
100	118	122	116	123
412	120	126	118	128
Temperature (°C)				
35	124	118	121	123
38	120	117	114	123
40	113	115	114	119
45	109	117	108	117

Fig. 11 Effect of zinc ion on cathodic polarization during zinc electrodeposition on an aluminum cathode in zinc electrolyte containing 170 g L^{-1} H$_2$SO$_4$, 12 g L^{-1} Mn^{2+} and 0.15 mg L^{-1} Pb^{2+}: **a** 12 g L^{-1} Mn^{2+} only, **b** 12 g L^{-1} Mn^{2+} and 0.15 mg L^{-1} Pb^{2+} at 40 °C with agitation of 60 rpm

Fig. 12 Effect of sulfuric acid on cathodic polarization during zinc electrodeposition on an aluminum cathode in zinc electrolyte containing 170 g L^{-1} H$_2$SO$_4$, 60 g L^{-1} Zn^{2+}, and **a** 12 g L^{-1} Mn^{2+} only or **b** 12 g L^{-1} Mn^{2+} and 0.15 mg L^{-1} Pb^{2+} at 40 °C and 60 rpm of agitation

increases the hydrogen diffusion more effectively in the double layer (Table 6). However, none of the mentioned parameters changed the mechanism of reduction according to the obtained values of the cathodic Tafel slopes.

3.4.2 Cyclic voltammetry study

Cyclic voltammetry was performed by scanning the potential from −1.30 to −0.70 V at 10 mV s^{-1}. This high scan rate was sufficient to determine the oxidation–reduction peaks. The voltammograms were initiated at point (A) (Figs. 13, 14) at a potential of −1.30 V, scanned in the positive direction, and then reversed at the potential −0.70 V in the negative direction, crossing over at point (B). No significant current was observed from point (C) until the potential reached point (B), corresponding to

the reduction of Zn^{2+} ions. The nucleation overpotential (NOP) is the difference between the crossover potential (B) (the start of the dissolution) and the point at which the Zn begins to deposit (D). Figure 13 shows the effect of sulfuric acid concentrations on the cyclic voltammogram of the aluminum electrode in zinc electrolyte containing 60 g L^{-1} Zn^{2+}, 12 g L^{-1} Mn^{2+}, and 0.15 mg L^{-1} Pb^{2+}. The NOP values were 50, 54, and 58 mV for 170, 165, and 158 g L^{-1} H$_2$SO$_4$, respectively. Increasing the sulfuric acid concentration decreased the NOP of the zinc deposit on the aluminum electrode.

Figure 14 shows the effect of different temperatures on the cyclic voltammogram of the aluminum electrode in zinc electrolyte containing 170 g L^{-1} H$_2$SO$_4$ and 60 g L^{-1} Zn^{2+}. The nucleation overpotentials of the zinc deposit on
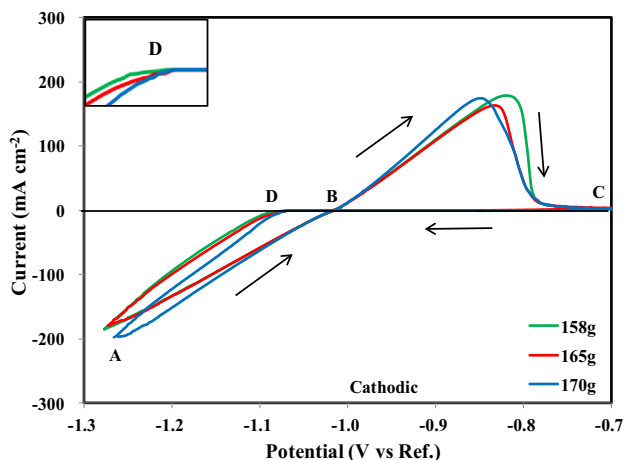
Fig. 13 Effect of different contents of sulfuric acid (158, 165, and 170 g L^{-1}) on the cyclic current–potential curves of the aluminum electrode in zinc electrolyte containing 60 g L^{-1} Zn^{2+}, 12 g L^{-1} Mn^{2+}, and 0.15 mg L^{-1} Pb^{2+} at 40 °C, no agitation and a scan rate of 10 mV s^{-1}
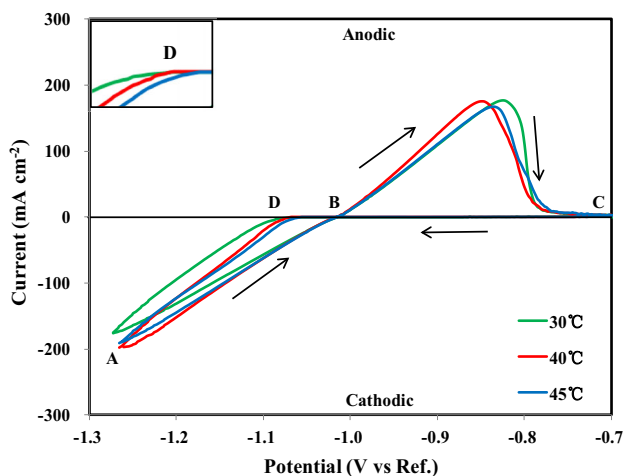

Fig. 14 Effect of different temperatures (35, 40, and 45 °C) on the cyclic current vs potential curve of the aluminum electrode in zinc electrolyte containing 170 g L^{-1} H$_2$SO$_4$, 60 g L^{-1} Zn^{2+}, 12 g L^{-1} Mn^{2+}, and 0.15 mg L^{-1} Pb^{2+} without agitation at a scan rate of 10 mV s^{-1}

the aluminum electrode from the curves are as follows: 56, 50, and 42 mV at 35, 40, and 45 °C, respectively. Increasing the electrolyte temperature decreased the nucleation overpotential of the zinc deposit on the aluminum electrode.
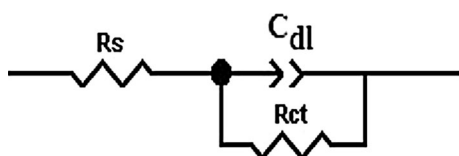
3.4.3 Electrochemical impedance spectroscopy

The impedance plots obtained at low potentials along the polarization curves (Fig. 15) resulted mainly in a high-frequency capacitive loop in the studied frequency domain.
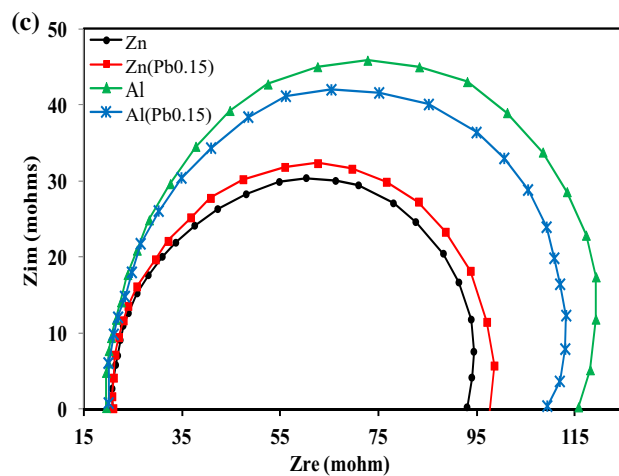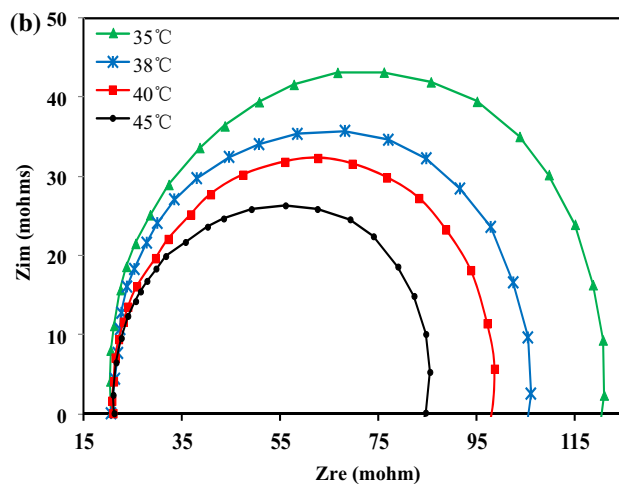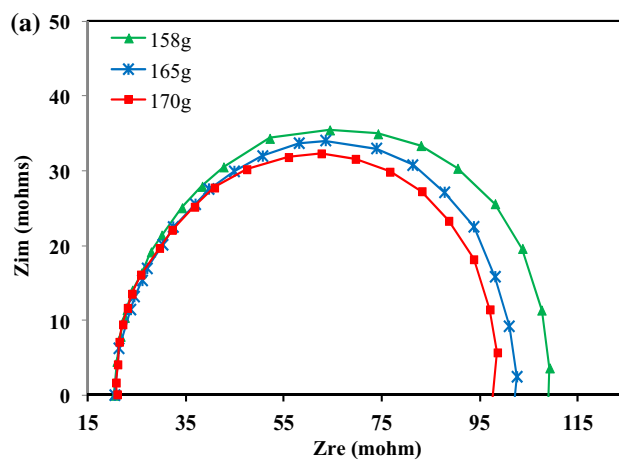
Fig. 15 Effect of concentrations of **a** sulfuric acid, **b** temperatures, and **c** lead content on Nyquist plots of the polarization resistances of the zinc deposit during zinc electrodeposition on the aluminum cathode and zinc cathodes in zinc electrolyte containing 60 g L^{-1} Zn^{2+} and 12 g L^{-1} Mn^{2+} at 40 °C and agitation of 60 rpm

This corresponds to the charge transfer resistance R_{ct}, of the zinc deposit in parallel with the double-layer capacitance C_{dl}.

Fig. 16 Equivalent circuit proposed for fitting the experimental data of electrochemical impedance measurements for the zinc deposit reaction on aluminum substrate

Figure 15 shows the effect of sulfuric acid concentrations, temperatures, and lead ions on Nyquist plots of the zinc deposit during zinc electrodeposition on the aluminum cathode and zinc cathodes in zinc electrolyte containing 60 g L^{-1} Zn^{2+} and 12 g L^{-1} Mn^{2+} at agitation of 60 rpm.

The equivalent circuit is presented in Fig. 16. R_S is the electrolyte resistance between the electrode surface and the salt bridge tip, R_{ct} is the charge transfer resistance of the zinc deposit in zinc electrolyte, and C_{dl} is the double-layer capacitance for the zinc deposit.

The solution resistance did not change and was always approximately 20 mΩ cm^2. The zinc deposit in the electrolyte containing 158 g L^{-1} H$_2$SO$_4$ had the highest charge transfer resistance (108.2 mΩ cm^2), followed by that of 165 g L^{-1} (95.6 mΩ cm^2), and 170 g L^{-1} (93.4 mΩ cm^2). As the temperature decreased, the resistance of charge transfer and C_{dl} decreased. R_{ct} decreased from 121.7 to 82.3 mΩ cm^2 as the temperature increased from 35 to 45 °C (Table 7). These results indicate that the reduction reactions are easier at higher temperatures and confirm the results obtained from potentiodynamic polarization. A high C_{dl} indicates that more electrons were adsorbed on the surface of the metal, indicating that low temperature resulted in an increase in overpotential during zinc deposition.

The values of charge transfer resistance (R_{ct}) and double-layer capacitance (C_{dl}) for zinc deposition on the zinc and aluminum cathodes in the presence of Pb^{2+} are shown in Table 8. Zinc reduction was easier on the zinc electrode

Table 7 Comparison of the parameters for the equivalent circuit of the zinc deposit reaction on aluminum cathodes during zinc electrodeposition

Parameter	R_s (mΩ cm^2)	R_{ct} (mΩ cm^2)	C_{dl} (mF cm^{-2})
H$_2$SO$_4$ (g L^{-1})			
158	20.3	108.2	24.3
165	20.5	95.6	26.4
170	21.0	93.4	94.1
Temperature (°C)			
35	20.6	121.7	103.8
38	20.5	105.8	98.6
40	21.0	93.4	94.1
45	21.2	82.3	85.3

than on the Al electrode. R_{ct} was 93.4 mΩ cm^2 in the case of Zn deposition on Zn and increased to 109.4 mΩ cm^2 for Zn deposition on Al. In addition, C_{dl} increased from 94.1 (Zn on Zn) to 99.7 mF cm^{-2} (Zn on Al cathode). The addition of Pb^{2+} ions increased R_{ct}, indicating that zinc reduction is more difficult in the presence of lead ions. This is confirmed by the C_{dl} value, which was 86.7 mF cm^{-2} for zinc deposition on the zinc substrate and increased to 90.6 mF cm^{-2} for zinc deposition on the Al substrate.

4 Conclusions

The effect of electrolyte composition and operating conditions of electrolysis on the overall performance of zinc deposition was evaluated. The following conclusions can be derived from this study:

1. Lead contamination of zinc deposits from the Pb–0.7wt.%Ag anode was approximately equivalent to that of soluble lead ions at a concentration of 0.15–0.2 mg L^{-1} Pb^{2+}. After 2 h of galvanostatic polarization employing a Pt anode with addition of 0.1–2.5 mg L^{-1} Pb^{2+} to the zinc electrolyte, the cathodic potential increased by 55 mV, and the current efficiency increased by 1.2%. With an electrolysis duration of up to 72 h, for both anodes, the cathodic potential decreased by ∼35 mV, and a decrease in the CE value of ∼6.8% was observed.

2. Addition of different concentrations of Mn^{2+} (4–16 g L^{-1}) to the electrolyte employing the Pb–Ag anode decreased the CE by 0.7–2% and shifted the cathodic potential to less negative values by 10–56 mV. In addition, a decrease in the lead content in the zinc deposit by 2.3–3.8 ppm was observed. A Mn^{2+} concentration of 12 g L^{-1} in the electrolyte could be considered an optimum level of manganese in the electrolyte since it gave a CE of 95.3%, with relatively low overpotential (45 mV), and reduced the lead contamination in the zinc deposit by 3.8 ppm. The detrimental effect of manganese ions addition could be due to the formation of MnO$_4^-$ ions, which accelerate the HER and decrease the rate of Zn^{2+} reduction.

3. Increasing the Zn^{2+} concentration from 56 to 65 g L^{-1} in the electrolyte increased the CE by ∼0.85% after 2 h of electrolysis. The cathodic potential was decreased by 13 mV for Pt and 18 mV for Pb–Ag. Increasing the acid concentration in the electrolyte from 158 to 170 g L^{-1} had a negative effect on the CE due to high hydrogen evolution, which hinders the reduction of Zn^{2+} ions.

4. Changing the current density from 45 to 60 mA cm^{-2} resulted in an increase in cathodic potential and an

Table 8 Comparison of the parameters for the equivalent circuit of the zinc deposit reaction on aluminum and zinc substrates in zinc electrolyte with and without 0.15 mg of Pb^{2+} additive measured by electrochemical impedance

Parameter	Zn	Zn (0.15 mg L^{-1} Pb^{2+})	Al	Al (0.15 mg L^{-1} Pb^{2+})
R_s (mΩ cm^2)	20.8	21.0	19.5	20.1
R_{ct} (mΩ cm^2)	93.4	98.6	109.4	115.7
C_{dl} (mF cm^{-2})	94.1	86.7	99.7	90.6

increase in current efficiency. Electrolyte agitation from 60 to 412 rpm resulted in reduced current efficiency and more negative overpotentials due to higher hydrogen mobility and the relatively slow reduction of zinc. The optimum value was 100 rpm; above this rate, the cathodic potential was almost stable, and the current efficiency decreased by only 0.4%.

5. Increasing the electrolyte temperature from 35 to 45 °C resulted in a decrease in the cathodic potential. The current efficiency was slightly increased by ∼0.3% as the temperature increased from 35 to 40 °C and increased sensitively by 0.8% from 40 to 45 °C. Generally, the influence of temperature is too complex to explain, especially for small changes. However, this could be due to the relatively more important effect on overpotential values and diffusion of Zn^{2+} than on the hydrogen reaction.

6. Electrochemical impedance spectroscopy confirmed the results of potentiodynamic polarization and cyclic voltammetry, showing that zinc reduction on the zinc electrode is easier than that on the aluminum electrode. R_{ct} was 93.4 mΩ cm^2 in the case of Zn deposition on deposited Zn and increased to 109.4 mΩ cm^2 for Zn deposition on Al cathode. C_{dl} increased from 94.1 to 99.7 mF cm^{-2}. The addition of Pb^{2+} ions increased R_{ct}, indicating that zinc reduction requires more overpotential in the presence of lead ions.

References

1. Sinclair RJ (2005) The extractive metallurgy of zinc. In: Sinclair R (ed), Australasian Institute of Mining and Metallurgy, pp 3–54
2. Alfantazi AM, Dreisinger DB (2001) The role of zinc and sulfuric acid concentrations on zinc electrowinning from industrial sulfate based electrolyte. J Appl Electrochem 3:641–646. doi:10.1023/A:1017569400346
3. Sorour N, Zhang W, Gabra G, Ghali E, Houlachi G (2015) Electrochemical studies of ionic liquid additives during the zinc electrowinning process. Hydrometallurgy 157:261–269. doi:10.1016/j.hydromet.2015.09.003
4. Ivanov I (2004) Increased current efficiency of zinc electrowinning in the presence of metal impurities by addition of organic inhibitors. Hydrometallurgy 72:73–78. doi:10.1016/S0304-386X(03)00129-4
5. Stefanov Y, Ivanov I (2002) The influence of nickel ions and tri-ethylbenzylammonium chloride on the electrowinning of zinc from sulphate electrolytes containing manganese ion. Hydrometallurgy 64:193–203. doi:10.1016/S0304-386X(02)00037-3
6. MacKinnon DJ, Brannen JM (1977) Zinc deposit structures obtained from high purity synthetic and industrial acid sulphate electrolytes with and without antimony and glue additions. J Appl Electrochem 7(5):451–459. doi:10.1007/BF00615950
7. Bozhkov C, Petrova M, Rashkov S (1990) The effect of nickel on the mechanism of the initial stages of zinc electrowinning from sulphate electrolytes. Part II. Investigations on aluminum cathodes alloyed with iron impurities. J Appl Electrochem 20:17–22. doi:10.1016/S1003-6326(08)60357-X
8. Mansfeld F, Gilman S (1970) The effect of lead ions on the dissolution and deposition characteristic of a zinc single crystal in 6 N KOH. J Electrochem Soc 117(5):588–592. doi:10.1149/1.2407584
9. Mackinnon DJ, Brannen JM, Kerby RC (1979) The effect of lead on zinc deposit structures obtained from high purity synthetic and industrial acid sulphate electrolytes. J Appl Electrochem 9:55–70. doi:10.1007/BF00620587
10. Zhang Q, Hua Y (2009) Effect of Mn^{2+} ions on the electrodeposition of zinc from acidic sulphate solutions. Hydrometallurgy 99:249–254. doi:10.1016/j.hydromet.2009.09.002
11. Hosny AY (1993) Electrowinning of zinc from electrolytes containing anti-acid mist surfactant. Hydrometallurgy 32:261–269. doi:10.1016/0304-386X(93)90029-D
12. Zhang Q, Hua Y, Dong T, Zhou D (2009) Effects of temperature and current density on zinc electrodeposition from acidic sulfate electrolyte with [BMIM] HSO4 as additive. J Appl Electrochem 39:1207–1216. doi:10.1007/s10800-009-9786-5
13. Tripathy BC, Das SC, Singh P, Hefter GT (1999) Zinc electrowinning from acidic sulphate solutions. Part III: effects of quaternary ammonium bromides. J Appl Electrochem 29:1229–1235. doi:10.1023/A:1003459822142
14. Scott AC, Pitblado RM, Barton GW (1987) A mathematical model of a zinc electrowinning cell. In: Proceedings of the twentieth international symposium on the application of computers and mathematics in the mineral industries, metallurgy, vol 2. pp 51–62
15. Bratt GC (1977) A view of zinc electrowinning theory. In: Proceedings of the AusI.M.M. conference, Tasmania. Australasian Institute of Mining and Metallurgy, Melbourne, Australia, pp 277–290
16. Fosnacht DR, O'Keefe TJ (1980) Evaluation of zinc sulphate electrolytes containing impurities and additives by cyclic

voltammetry. J Appl Electrochem 10:495–504. doi:10.1007/BF00614083

17. Hosny AY, O'Keefe TJ, Johnson JW, James WJ (1991) Correlation between mass transfer and operating parameters in zinc electrowinning. J Appl Electrochem 21(9):785–792. doi:10.1007/BF01402815

18. Ivanov I, Stefanov Y (2002) Electroextraction of zinc from sulphate electrolytes containing antimony ions and hydroxyethylated-butyne-2-diol-1,4: part 3. The influence of manganese ions and a divided cell. Hydrometallurgy 64:181–186. doi:10.1016/S0304-386X(02)00039-7

19. Tswuoka T (1960) Behaviour of manganese in the electrodeposition of zinc. Nippon Kogyo Kaishi 76:311–318

20. Milazzo G (1969) Électrochimie, Tome 1: Bases Théoriques. Applications Analytiques Électrochimie des Colloïdes. Dunod, Paris, pp 150–151

21. Fukubayashi H (1972) The effect of impurities and additives on the electrowinning of zinc. Doctoral Dissertations, University of Missouri, pp 41–50

22. Barton GW, Scott AC (1992) A validated mathematical model for a zinc electrowinning cell. J Appl Electrochem 22(2):104–115. doi:10.1007/BF01023811

23. Kelly RB, Scually JR, Shoesmith DV, Buchheit RG (2002) Electrochemical techniques in corrosion science and engineering. CRC Press, New York, p 53

24. Fletcher S (2009) Tafel slopes from first principles. J Solid State Electrochem 13:537–549. doi:10.1007/s10008-008-0670-8